

RESEARCH

Open Access



# Proteomic analysis implicates that postovulatory aging leads to aberrant gene expression, biosynthesis, RNA metabolism and cell cycle in mouse oocytes

Chuanxin Zhang<sup>1</sup>, Xueqi Dong<sup>1</sup>, Xinyi Yuan<sup>1</sup>, Jinzhu Song<sup>1</sup>, Jiawei Wang<sup>1</sup>, Boyang Liu<sup>1</sup> and Keliang Wu<sup>1\*</sup>

## Abstract

**Background** In mammals, oocytes display compromised quality after experiencing a process of postovulatory aging. However, the mechanisms underlying are not yet fully understood. Here, we portrayed a protein expression profile of fresh and aging metaphase II (MII) mouse oocytes by means of four-dimensional label-free quantification mass spectrometry (4D-LFQ).

**Results** The analysis of 4D-LFQ data illustrated that there were seventy-six differentially expressed proteins (DEPs) between two groups of MII stage oocytes. Fifty-three DEPs were up-regulated while twenty-three DEPs were down-regulated in the MII oocytes of the aging group, and Gene Ontology (GO) analysis revealed that these DEPs were mainly enriched in regulation of gene expression, biosynthesis, RNA metabolism and cell cycle. Our detailed analysis revealed that the expression of proteins that related to gene expression processes such as transcription, translation, post-translational modifications and epigenome was changed; the relative protein expression of RNA metabolic processes, such as RNA alternative splicing, RNA export from nucleus and negative regulation of transcription from RNA polymerase II promoter was also altered.

**Conclusion** In conclusion, we identified considerable DEPs and discussed how they agreed with previous researches illustrating altered protein expression associated with the quality of oocytes. Our research provided a new perspective on the mechanisms of postovulatory aging and established a theoretical support for practical methods to control and reverse postovulatory aging.

**Keywords** Postovulatory aging, Proteomics, Epigenome, Biosynthesis, RNA alternative splicing, Cell cycle

\*Correspondence:

Keliang Wu  
wukeliang\_527@163.com

<sup>1</sup>Center for Reproductive Medicine, Shandong University, 250012 Jinan, Shandong, China



© The Author(s) 2022. **Open Access** This article is licensed under a Creative Commons Attribution 4.0 International License, which permits use, sharing, adaptation, distribution and reproduction in any medium or format, as long as you give appropriate credit to the original author(s) and the source, provide a link to the Creative Commons licence, and indicate if changes were made. The images or other third party material in this article are included in the article's Creative Commons licence, unless indicated otherwise in a credit line to the material. If material is not included in the article's Creative Commons licence and your intended use is not permitted by statutory regulation or exceeds the permitted use, you will need to obtain permission directly from the copyright holder. To view a copy of this licence, visit <http://creativecommons.org/licenses/by/4.0/>. The Creative Commons Public Domain Dedication waiver (<http://creativecommons.org/publicdomain/zero/1.0/>) applies to the data made available in this article, unless otherwise stated in a credit line to the data.

## Background

It is well known that mammals oocytes are the foundation of reproductive biology. Mature oocytes stagnated at meiotic metaphase II (MII) are fertilized in an optimal time window after ovulation, namely 8–12h for mice and within 24h for humans [1]. Otherwise, it undergoes a time-dependent process of deterioration in the oviduct (in vivo) or culture media (in vitro) regarded as postovulatory aging [2, 3]. The degradation of oocyte quality due to postovulatory aging was associated with decreased fertilization rates, compromised embryo quality, implantation failure, early abortion and the birth of unhealthy offspring in various species [4–8].

A diverse variety of undesirable variations were demonstrated in the aging oocytes, including zona pellucida hardening, organellar dysfunction, spindle and chromosome abnormalities and aberrant regulation of molecular and biochemical events [6, 9]. Although in vivo and in vitro postovulatory aging resemble each other in manifestations, in vitro postovulatory aging leads to more extreme alterations on oocytes as the culture medium does not fully mimic the in vivo environment [6]. Accumulating evidences showed that oxidative stress [5, 10], altered Ca<sup>2+</sup> homeostasis [1, 11], deadenylation of poly(A) tails of maternal effect genes [12] and epigenomic aberrations [13] were involved in the aging process. However, the precise molecular causes account for the series of changes in postovulatory aging oocytes remain to be further elucidated.

Since protein is the executor of vital biological processes, the variation of protein abundance plays an important role in the embryonic development [14]. A considerable series of correlative processes are demanded to maintain the abundance of cellular proteins, spanning the transcription, post-transcriptional processing and degradation of mRNAs to the translation, posttranslational modification and destruction of the proteins themselves [15–17]. Previous study by Jia, Bao-Yu et al. revealed that the function of endoplasmic reticulum and Golgi apparatus, two important organelles that play an important role in protein synthesis and processing, was significantly impacted in the aging oocytes. Thus, we supposed that the abundance of proteins in the aging oocytes may be broadly disturbed [2]. In order to comprehensively explore the molecular mechanisms of postovulatory aging, it has become an inevitable trend of current research to detect protein expression levels.

Mass spectrometry (MS) has become one of the major tools to detect and quantify a large quantity of proteins. The last few years have seen the birth of 4D-LFQ, a momentous breakthrough in proteomics technology. Apart from time, m/z and ion strength, the incorporation of ion mobility as an additional separation dimension into MS significantly improves the sensitivity of the

measurement [18, 19]. Meanwhile, the application of parallel accumulation serial fragmentation (PASEF) greatly improves the scanning speed. The high sensitivity and speed of trapped ion mobility quadrupole time-of-flight mass spectrometer (timsTOF Pro) allow us to drastically increase measurement throughput and decrease sample amount, especially suitable for the detection of limited sample amounts and has been applied to tear fluid, plasma, sporozoite and so on. [19–21]. However, this technology has never been conducted on oocytes before. Considering that in vitro postovulatory aging can be easily influenced by the ingredients of culture media, in the current study, we performed the 4D-LFQ on in vivo postovulatory aging mouse oocytes model for the first time to map the dynamic proteomic changes between fresh and aging oocytes of mouse.

## Materials and methods

### Oocyte collection

Mice of Institute of Cancer Research (ICR) breed bought from Beijing Weitong Lihua Co., LTD were cultivated under standard conditions (12h dark and 12h light cycle, food and water ad libitum) in this experiment. To induce superovulation, 6- to 8- week-old female mice were injected intraperitoneally with 5 IU pregnant mare serum gonadotropin (PMSG) (110,914,564, Ningbo Sansheng Biological Technology Co., LTD), followed by 5 IU human chorionic gonadotropin (hCG) (110,911,282, Ningbo Sansheng Biological Technology Co., LTD) 48h later. The superovulated mice were humanly sacrificed at 13 and 25h after hCG injection, and the cumulus oocyte complexes (COCs) released from the oviductal ampullae were denuded of cumulus cells by pipetting with a thin pipette in a drop of M2 medium (M7167; Sigma-Aldrich) containing 0.1% hyaluronidase (H3506; Sigma-Aldrich) and collected as fresh and aging oocytes respectively.

### Protein extraction and trypsin digestion

The zona pellucida of oocytes was removed with acid Table's solution (MR-004-D, Sigma-Aldrich) and washed with PBS (KGB5001, keyGEN bioTECH). The oocytes were transferred to a 1.5mL centrifuge tube, and 100 oocytes were collected as a group. The aging and fresh oocytes were both collected for three biological replicates, refrigerated at -80°C, shipped on dry ice.

Samples were taken out from -80°C, a certain volume of lysis buffer consist of 8M urea (Sigma-Aldrich, USA) and 1% Protease Inhibitor Cocktail (Merck Millipore, Germany) was added, followed by sonication via ultrasound. The samples were centrifuged at 12,000×g at 4°C for 10min and the cell fragments were removed. The supernatant was transferred to a new centrifuge tube. An appropriate volume was taken and directly dyed with silver glue (Solarbio, China).

For digestion, the protein solution was reduced with 5mM dithiothreitol (Sigma-Aldrich, USA) for 30min at 56°C and alkylated with 11mM iodoacetamide (Sigma-Aldrich, USA) for 15min at room temperature in darkness. The sample was then diluted by adding 100mM TEAB (Sigma-Aldrich, USA) till urea concentration was less than 2M. Finally, trypsin (Promega, USA) was added at a 1:50 trypsin-to-protein mass ratio overnight and then a 1:100 trypsin-to-protein mass ratio for 4h.

#### Liquid chromatography-mass spectrometry analysis and database search

The tryptic peptides were dissolved in 0.1% formic acid and 2% acetonitrile (solvent A) and separated by NanoE-lute ultra-high performance liquid system. The gradient consisted of an increase from 6 to 24% solvent B (0.1% formic acid in 100% acetonitrile) in 70min, 24–35% in 14min and climbing to 80% in 3min then holding at 80% for the last 3min, all at a constant flow rate of 450 nL/min. The peptides were injected into Capillary ion source for ionization at 2.0kV and analyzed by timsTOF Pro mass spectrometry. The peptide parent ions and their secondary fragments were detected and analyzed using high-resolution TOF. The *m/z* scan range was 100–1700 for full scan. After a first-order mass spectrometry collection, the secondary spectra with the charge number of parent ions in the range of 0–5 were collected in parallel cumulative serial fragmentation (PASEF) mode for 10 times with 30s dynamic exclusion.

The Secondary mass spectrometry data were retrieved using the Maxquant search engine (v.1.6.15.0) from the Mus\_musculus\_10090 database concatenated with the reverse decoy database. Trypsin/P was set as a cleavage enzyme and the number of missing cleavages was set as 2. The mass tolerance for precursor ions was set as 20 ppm in the first search and 20 ppm in the main search, and the mass tolerance for fragment ions was set as 20 ppm. Carbamidomethyl on Cys was set as a fixed modification and acetylation modification and oxidation on Met were set as variable modifications. The false discovery rate (FDR) was specified as 1%, and the minimum length for modified peptides was set as 7.

The expression values of each protein were calculated as the expected number of fragments per kilobase of transcript sequence per millions base pairs sequenced (FPKM). When  $p\text{-value} \leq 0.05$  and  $\text{fold change} > 1.5$ , the protein would be considered differentially expressed. Gene Ontology (GO, <http://www.geneontology.org/>) analysis, Kyoto Encyclopedia of Genes and Genomes (KEGG, <http://www.kegg.jp/>) analysis and eukaryote clusters of orthologous groups (KOG, <http://www.ncbi.nlm.nih.gov/COG>) classification of the enrichment of DEPs were performed. An adjusted  $P\text{-value} < 0.05$  indicated the significant protein enrichment.

#### Immunofluorescence microscopy

In general, at room temperature, oocytes were fixed with 4% paraformaldehyde in PBS for 30min, and permeabilized with 0.3% Triton-100 (T8787, Sigma-Aldrich) in PBS for 20min, then blocked with 1% BSA (0332, amresco) in PBS containing 0.1% Tween-20 (P9416, Sigma-Aldrich) and 0.01% Triton – 100 for 30min. Next, oocytes were incubated with primary antibodies in 1% BSA for 1h. After being washed three times in PBS containing 0.1% Tween-20 and 0.01% Triton – 100 with each time for 5min, oocytes were incubated with secondary antibody in PBS containing 0.1% Tween-20 and 0.01% Triton – 100 for 30min. Similarly, after being washed three times, oocytes were transferred onto slides in PBS containing 0.1% Tween-20 and 0.01% Triton – 100 and detected under a laser scanning confocal microscope (Dragonfly, Andor Technology, UK).

The primary antibodies were listed as follows: MTX2 (1:100 in dilution, 11610-1-AP, Proteintech), GDF9 (1:100 in dilution, ab93892, Abcam), TACC3 (1:50 in dilution, ab134154, Abcam), EIF5A (1:50 in dilution, 11309-1-AP, Proteintech), ASPM (1:150 in dilution, 26223-1-AP, Proteintech). The secondary antibodies were presented as follows: Goat Anti-Rabbit IgG H&L (Alexa Fluor 488) preadsorbed (1:500 in dilution, ab150081, Abcam), Goat Anti-Rabbit IgG H&L (Alexa Fluor 594) (1:500 in dilution, ab150080, Abcam), DAPI (1:500 dilution, D3571, Life Technologies).

#### Statistical analysis

Images of oocytes labeled with the same antibody were captured under the identical scan setups. The mean fluorescence intensity in each oocyte was measured using ImageJ software (National Institutes of Health, Bethesda, MD, USA). Fluorescence values of fresh oocytes were arbitrarily set as 1, and values of aging oocytes were fixed relative to that of the fresh oocytes. The results were described as the mean  $\pm$  SEM (standard error of mean). Statistical comparisons were performed using two-tailed Student's *t*-test or Chi-square test.  $P\text{-values} < 0.05$  were considered significant (\* $p < 0.05$ ; \*\* $p < 0.01$ ; \*\*\* $p < 0.001$ ).

## Results

### Global proteomics characteristics between fresh and aging mouse oocytes

In this study, mouse oocytes collected 13h after hCG injection were regarded as fresh oocytes while those obtained 25h after hCG injection were seen as aging oocytes. To determine the differences in protein expression between fresh and aging oocytes, three biological replicates of each group were subjected to 4D-LFQ. First, principal component analysis was used to assess the protein intra-group repeatability. The results of biological and technical replicates were statistically consistent,

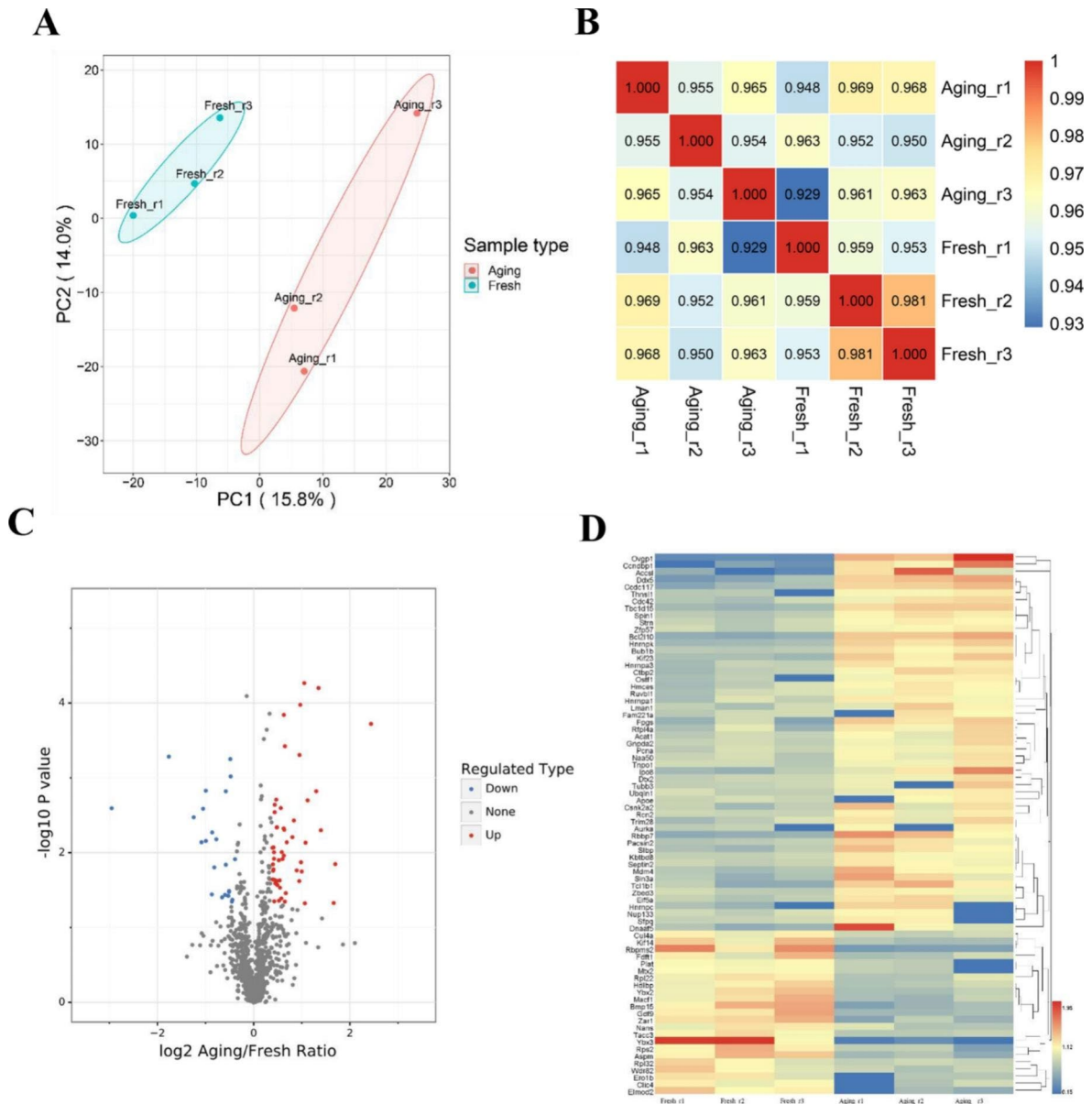


**Fig. 1** Protein expression levels of fresh and aging mouse MII oocytes. **a** Quantitative principal component analysis of all samples of fresh and aging oocytes. **b** Spearman's correlation heatmap showing the consistency between repetitive samples and the discrepancy between groups. Color gradient indicates the magnitude of the correlation coefficient. **c** DEPs between oocytes of Fresh and Aging are shown in the volcano map. Proteins that express higher (up-regulated) in aging oocytes are shown in red, and proteins that are lower (down-regulated) are shown in blue. **d** Expression profiles heatmap of 76 DEPs in fresh and aging oocytes with a color gradient for gene abundance ranks

and the aging oocytes were clearly distinguished from the fresh group (Fig. 1A). The spearman correlation coefficients between biological replicates were greater than 0.95, indicating that the biological repeat of mass spectrum (MS) exhibited highly reproducible results (Fig. 1B). A total of 11,438 peptides were identified by spectrogram analysis, among which 11,089 were specific peptides. According to this criterion, the total protein number identified was 1,887, of which 1,266 were quantifiable. The details of all identified proteins as well as the peptides were provided in Table S1. Subsequently, totally

seventy-six differentially expressed proteins (DEPs) were screened out by log<sub>2</sub> (Fold Change) greater than 1.3, among which 53 were up-regulated and 23 down-regulated (Fig. 1C and 1D). Therefore, we found that aging oocytes possessed a significantly different protein expression patterns compared with fresh oocytes.

To verify the proteomics results, samples of both fresh and aging oocytes were further analyzed by immunofluorescence. We chose metaxin-2 (MTX2), growth/differentiation factor 9 (GDF9), transforming acidic coiled-coil-containing protein 3 (TACC3), eukaryotic

translation initiation factor 5A-1 (EIF5A) and abnormal spindle-like microcephaly-associated protein homolog (ASPM) as candidates in the experiment, and the results were consistent with the 4D-LFQ analysis (Fig. 2A-F).

#### GO, KEGG and KOG analysis of DEPs for fresh and aging oocytes

To better understand the functions the DEPs performed during postovulatory aging, the DEPs were enriched into GO terminology. GO analysis showed that alterations of protein expression were related to manifold biological processes, cellular components and molecular functions (Fig. 3A). “Cellular process” and “biological regulation” were revealed with salient differences in biological processes category, including 56 and 52 DEPs, respectively. “Cell” and “organelle” were shown to be interfered in cellular components category, involving 65 and 56 DEPs, respectively. “Binding” and “catalytic activity” showed a significantly close relationship in molecular functions category, including 51 and 24 DEPs, respectively. In terms of biological processes, the most enriched GO terms fell into four major classes, regulation of gene expression, regulation of biosynthetic process, regulation of RNA metabolic process and regulation of cell cycle process, which were the main focuses in the subsequent parts (Fig. 3B). For cellular components, the two most enriched terms were intracellular non-membrane-bounded organelle and non-membrane-bounded organelle (Fig. 3C). And as to molecular functions, protein domain specific binding was the most enriched term (Fig. 3D).

The Kyoto Encyclopedia of Genes and Genomes (KEGG) classification system serves as an alternative functional annotation of proteins in accordance with their related biochemical pathways. Regardless of whether the protein was up-regulated or down-regulated, the most significant enrichment was the “spliceosome” pathway (Fig. 4A).

To further verify the effectiveness of the annotation process, we identified the unigene numbers with eukaryote clusters of orthologous groups (KOG) classification. Altogether, there were 69 unigenes identified to 18 categories (Fig. 4B). Among these categories, “RNA processing and modification” and “Signal transduction mechanism” accounted for the largest proportion (8, 11.6%) followed by “Intracellular trafficking, secretion, and vesicular transport” and “cytoskeleton” (7, 10.1%), and then “transcription” (6, 8.7%).

#### Abnormal regulation of gene expression during the process of postovulatory aging

In order to function accurately and timely, oocyte strictly regulates its gene expression to meet the specific protein demands at given moments. Briefly, there are three major stages along the protein production pathway that

an oocyte can perform gene regulation: transcription, translation and post-translational modifications respectively [22]. Among DEPs related to regulation of gene expression, twenty were annotated with regulation of “transcription” associated GO terms including DEAD box helicase 5 (DDX5), heterogeneous nuclear ribonucleoprotein K (Hnrnpk) and so on; four were annotated with “regulation of translation” GO term including Eif5a, aurora kinase A (Aurka), Y-box-binding protein 2 (Ybx2) and Y-box-binding protein 3 (Ybx3); and two were annotated with “post-translational protein modification” GO term including retinoblastoma binding protein 7, chromatin remodeling factor (RBBP7) and bone morphogenetic protein 15 (Bmp15), indicating all stages of gene regulation were influenced by postovulatory aging (Fig. 5A-C).

Meanwhile, establishment of the epigenetic asset also plays an essential role in the preservation of cell identity and the regulation of gene expression, which is indispensable for normal development after fertilization. [1, 23]. In our study, eight up-regulated DEPs were found to be related with epigenetic modification based on “histone modification”, “methylation” or epigenetic-associated GO terms, including RBBP7, transcriptional regulator, SIN3A (Sin3a), tripartite motif-containing 28 (Trim28), Aurka, zinc finger protein 57 (Zfp57), splicing factor proline/glutamine rich (Sfpq), stem-loop binding protein (SLBP) and RuvB-like 1 (Ruvbl1) (Fig. 5D).

#### Interference in regulation of RNA metabolic process during the process of postovulatory aging

By information retrieval using the National Center for Biotechnology Information (NCBI) [24], we initially divided the up-regulated proteins related to regulation of RNA metabolic process into three categories: RNA alternative splicing, RNA export from nucleus and negative regulation of transcription from RNA polymerase II promoter, respectively (Fig. 6A-C). Among these proteins, five DEPs were splicing-related proteins based on “RNA splicing” or spliceosome-associated GO terms [25], including Ddx5, Hnrnpc, Hnrnpk, heterogeneous nuclear ribonucleoprotein A1 (Hnrnpa1) and Sfpq (Fig. 6A); three DEPs participated in RNA export from nucleus including Slbp, Hnrnpa1 and nucleoporin 133 (Nup133) (Fig. 6B); eight DEPs functioned in negative regulation of transcription from RNA polymerase II promoter, respectively Ddx5, Rbbp7, Hnrnpk, Sfpq, Trim28, Zfp57, proliferating cell nuclear antigen (Pcna) and transformed mouse 3T3 cell double minute 4 (Mdm4) (Fig. 6C).

The seven down-regulated proteins associated with “regulation of RNA metabolic process” GO term were presented in Fig. 6D. It is worth noting that the abundance of the germ-cell specific RNA-binding protein YBX2 (also known as MSY2), which plays a central role

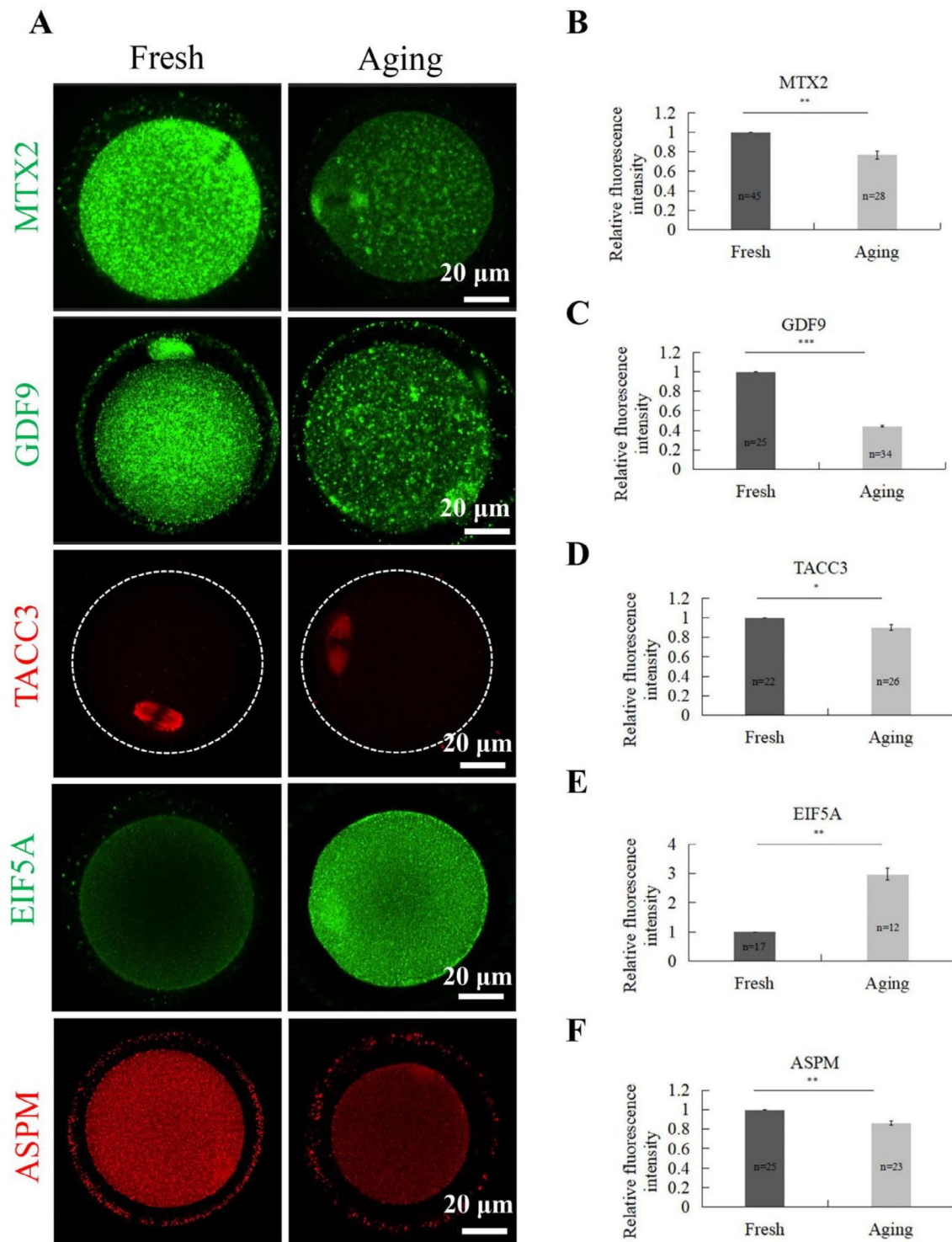


**Fig. 2** Validation of DEPs by immunofluorescence. **a** Representative confocal images of fluorescent staining of five candidate DEPs in fresh and aging oocytes, namely MTX2, GDF9, TACC3, EIF5A and ASPM. Scale bar, 20 $\mu$ m. **b** Intracellular relative fluorescence intensity of MTX2 signal intensity in fresh and aging oocytes. **c** Intracellular relative fluorescence intensity of GDF9 signal intensity in fresh and aging oocytes. **d** Intracellular relative fluorescence intensity of TACC3 signal intensity in fresh and aging oocytes. **e** Intracellular relative fluorescence intensity of EIF5A signal intensity in fresh and aging oocytes. **f** Intracellular relative fluorescence intensity of ASPM signal intensity in fresh and aging oocytes. \* $p < 0.05$ , \*\* $p < 0.01$ , \*\*\* $p < 0.001$  indicate significant differences

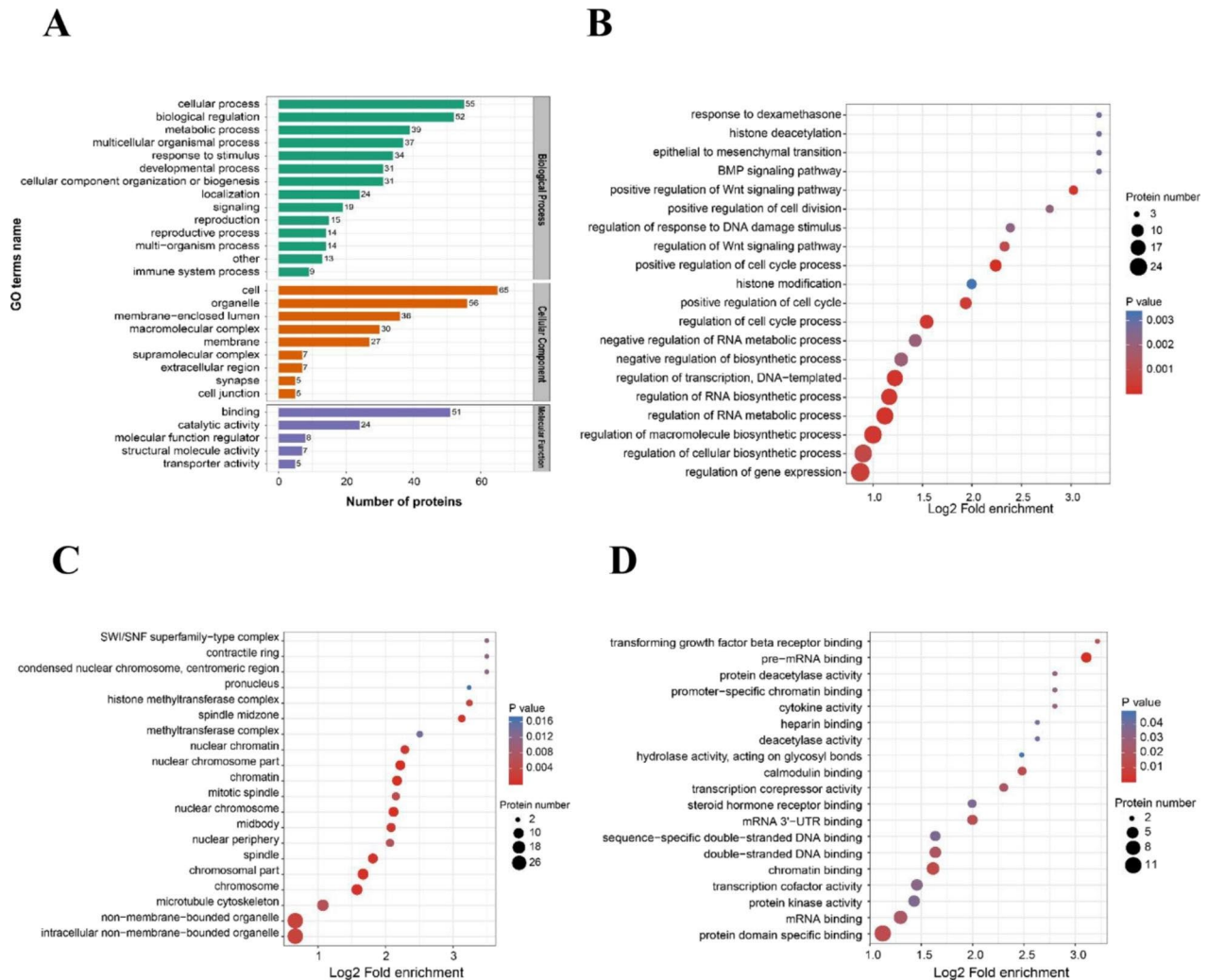


**Fig. 3** GO analysis of differentially expressed proteins (DEPs) between fresh and aging mouse MII oocytes. **a** GO (Gene Ontology) enrichment analysis on DEPs. Green refers to terms relating to biological processes, orange refers to terms relating to cellular components and purple refers to terms relating to molecular function. **b** The top 20 GO terms related to biological process were presented in the enrichment analyses of DEPs within the aging oocytes. **c** The top 20 GO terms related to cellular components were presented in the enrichment analyses of DEPs within the aging oocytes. **d** The top 20 GO terms related to molecular function were presented in the enrichment analyses of DEPs within the aging oocytes

in ensuring the stability of mRNAs and their poly(A) tail [26], was significantly reduced.

Taken together, our analyses suggest that postovulatory aging has a differential influence on RNA splicing, RNA export from nucleus, transcription and RNA stability, which appears to be one of the causes of declined quality and developmental potential in the aging oocytes.

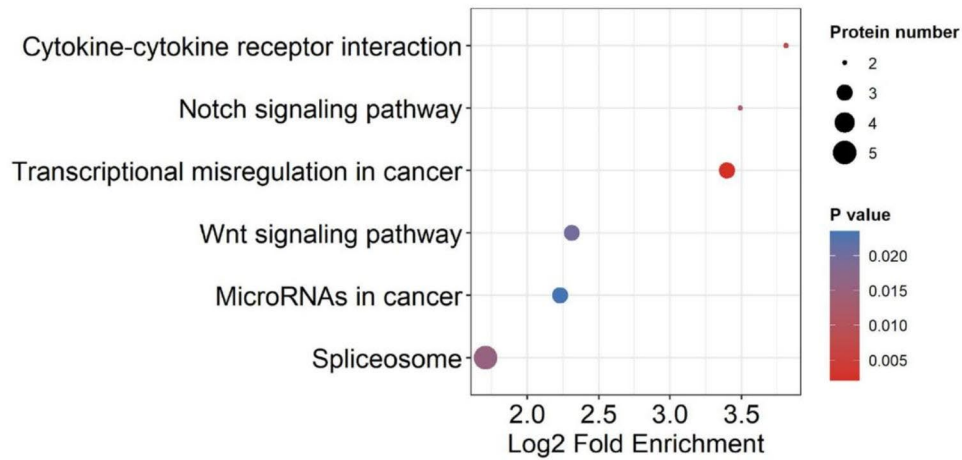
#### Altered regulation of biosynthetic process and cell cycle process due to postovulatory aging

Apart from an important maternal genetic contribution to each progeny, oocytes also provide a large library of macromolecules for offspring to maintain early embryogenesis and control necessary metabolic functions [27, 28]. Intriguingly, a total of 33 proteins differentially expressed were biosynthesis-related based on “regulation

of biosynthetic process” associated GO terms, among which twenty-two showed an increased expression pattern, while eleven exhibited a reduced expression level (Fig. 7A). Among these DEPs, there were two pivotal oocyte-secreted factors, Gdf9 and Bmp15, both of which belong to the transforming growth factor-beta (TGF $\beta$ ) superfamily. It has been reported that the combination of Gdf9 and Bmp15 acts as activator in the process of steroidogenesis [29]. The down regulation of the two proteins might interfere with the synthesis of steroid hormones and thus disrupt the endocrine and paracrine communications between cumulus cells and the oocyte.

Numerous cell cycle-related defects were observed in the aging oocytes including abnormal length of spindle, depolymerized astral microtubules, chromosomal misalignments, premature chromosome separation and so

**A**



**B**

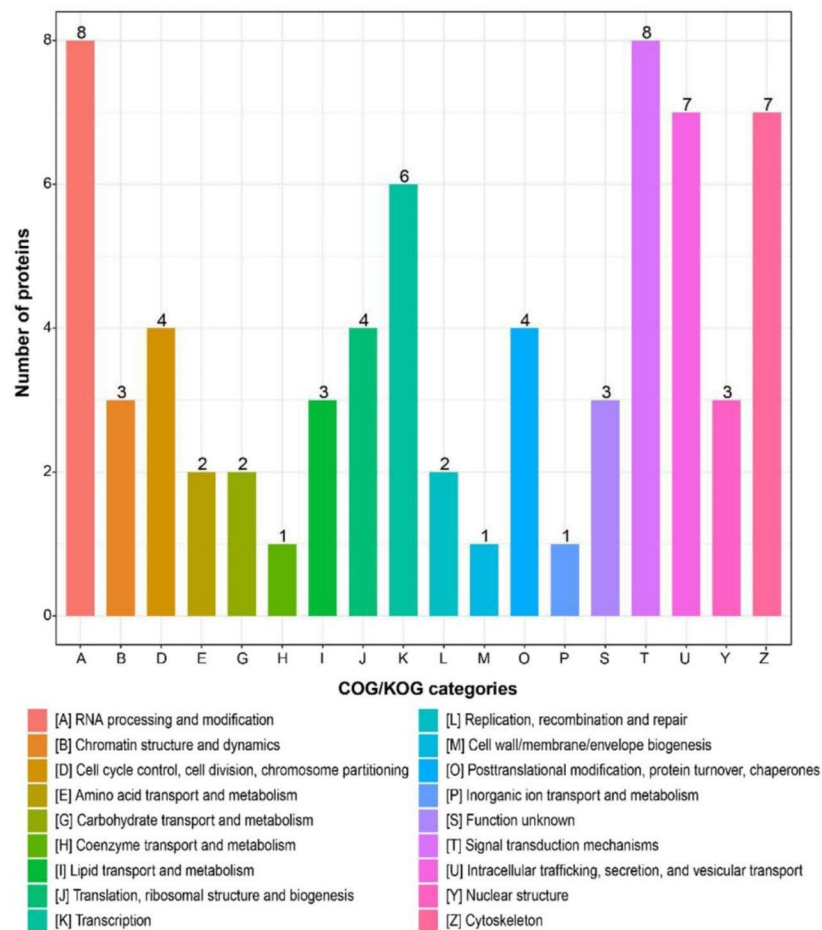


**Fig. 4** KEGG and KOG analysis of differentially expressed proteins (DEPs) between fresh and aging mouse MII oocytes. **a** The top KEGG pathways were presented in the enrichment analyses of DEPs within the aging oocytes. **b** Histogram representing clusters of orthologous groups (KOG) classification. The legend on the bottom showed a description of the 18 functional categories



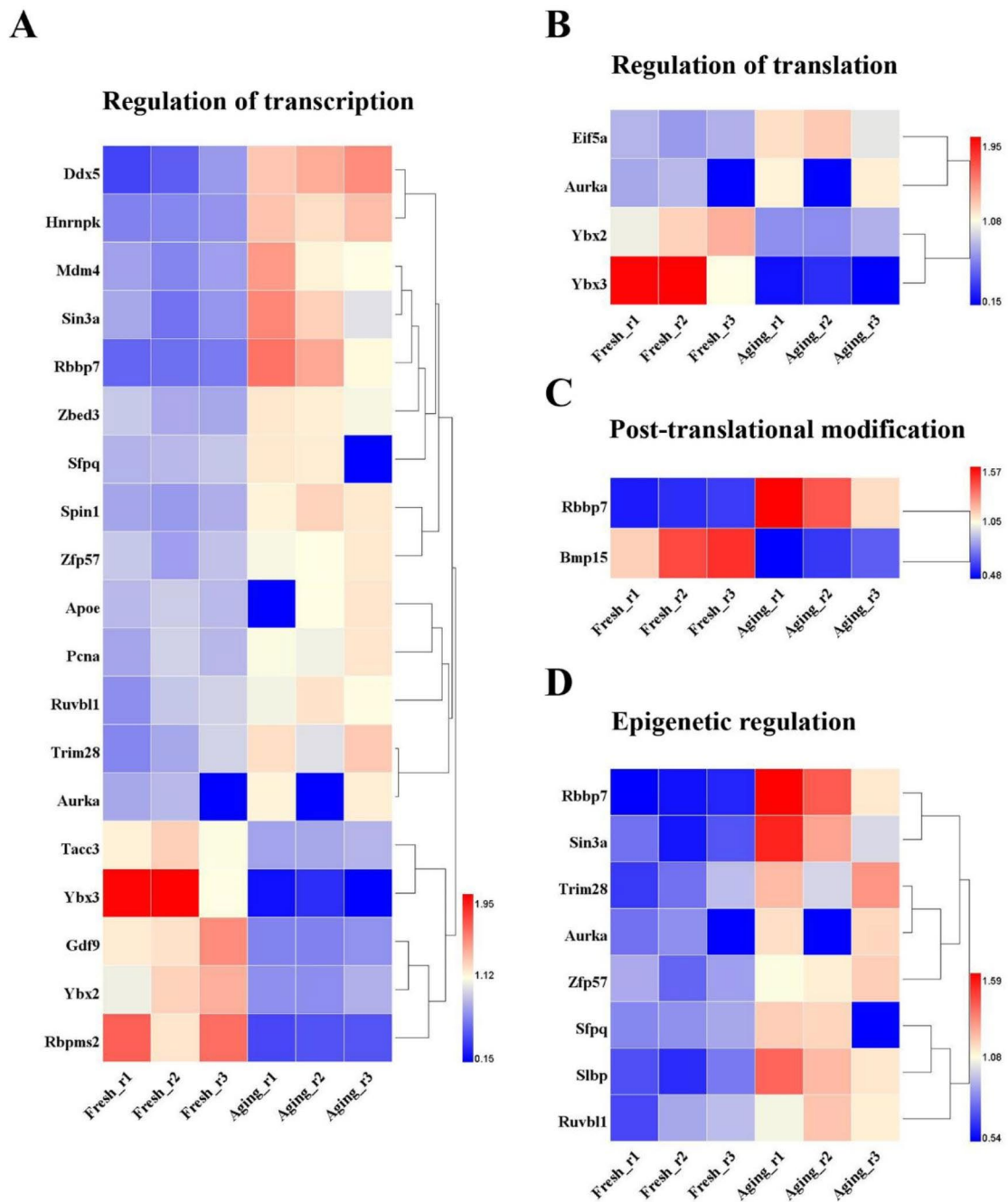


**Fig. 5** Abnormal regulation of gene expression during the process of postovulatory aging. **a** The heat map for the protein expression level related to the regulation of transcription. **b** The heat map for the protein expression level related to the regulation of translation. **c** The heat map for the protein expression level related to the regulation of post-translational modification. **d** The heat map for the protein expression level related to the epigenetic regulation

on [1, 9]. Likewise, we found that up to 19 proteins differentially expressed were involved in regulation of cell cycle. Fifteen of them were up-regulated, while only four showed a decreased expression pattern (Fig. 7B).

**Discussion**

The declining quality of oocytes due to postovulatory aging is a major problem in reproductive medicine as fertilization of obtained mature oocytes can be postponed on account of various unforeseeable circumstances such as increased workload or delayed accessibility of semen samples [2, 6]. Therefore, significant importance should

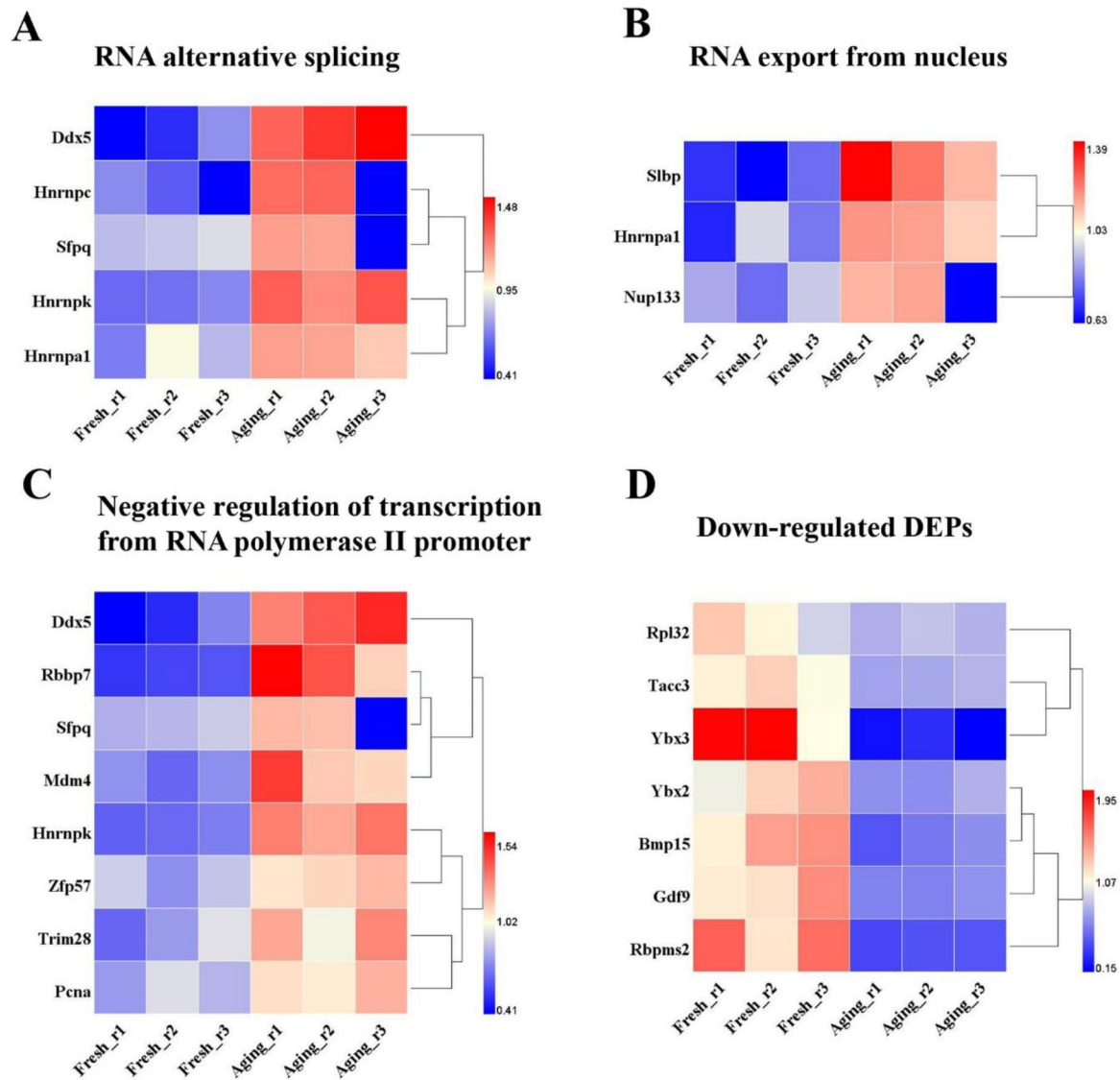


**Fig. 6** Interference in regulation of RNA metabolic process during the process of postovulatory aging **a** The heat map for the protein expression level related to RNA alternative splicing. **b** The heat map for the protein expression level related to RNA export from nucleus. **c** The heat map for the protein expression level related to negative regulation of transcription from RNA polymerase II promoter. **d** The heat map for the down-regulated protein expression level related to the regulation of RNA metabolic process

be attached to figure out the underlying mechanisms and potential methods to control and reverse the process. Taking it into account that protein is the ultimate executor of molecular functions, we conducted 4D-LFQ to investigate the protein expression profile alterations during mice postovulatory aging.

A total of 1266 quantitative proteins were identified in this study. Among the 76 proteins (6%) that were significantly differentially expressed, 53 (4.2%) showed up-regulation expression in the aging group while 23 (1.8%) were downregulated. Compared to previous study by Jiang et al. a decade ago, which reported 26 DEPs in

vitro in aging porcine oocytes using two-dimensional Difference Gel Electrophoresis (2D DIGE) together with Matrix-Assisted Laser Desorption/Ionization Time of Flight/Time of Flight Mass Spectrometry (MALDITOF-TOF MS) [30], we identified significantly more DEPs with more advanced 4D-LFQ technology, let alone that more DEPs, varying with different culture media, should be found refer to in vitro postovulatory aging. To further understand the impact of postovulatory aging on oocytes, the DEPs were enriched into the GO, KEGG and KOG analysis, starting with biological processes, cellular components and molecular functions, pathways and

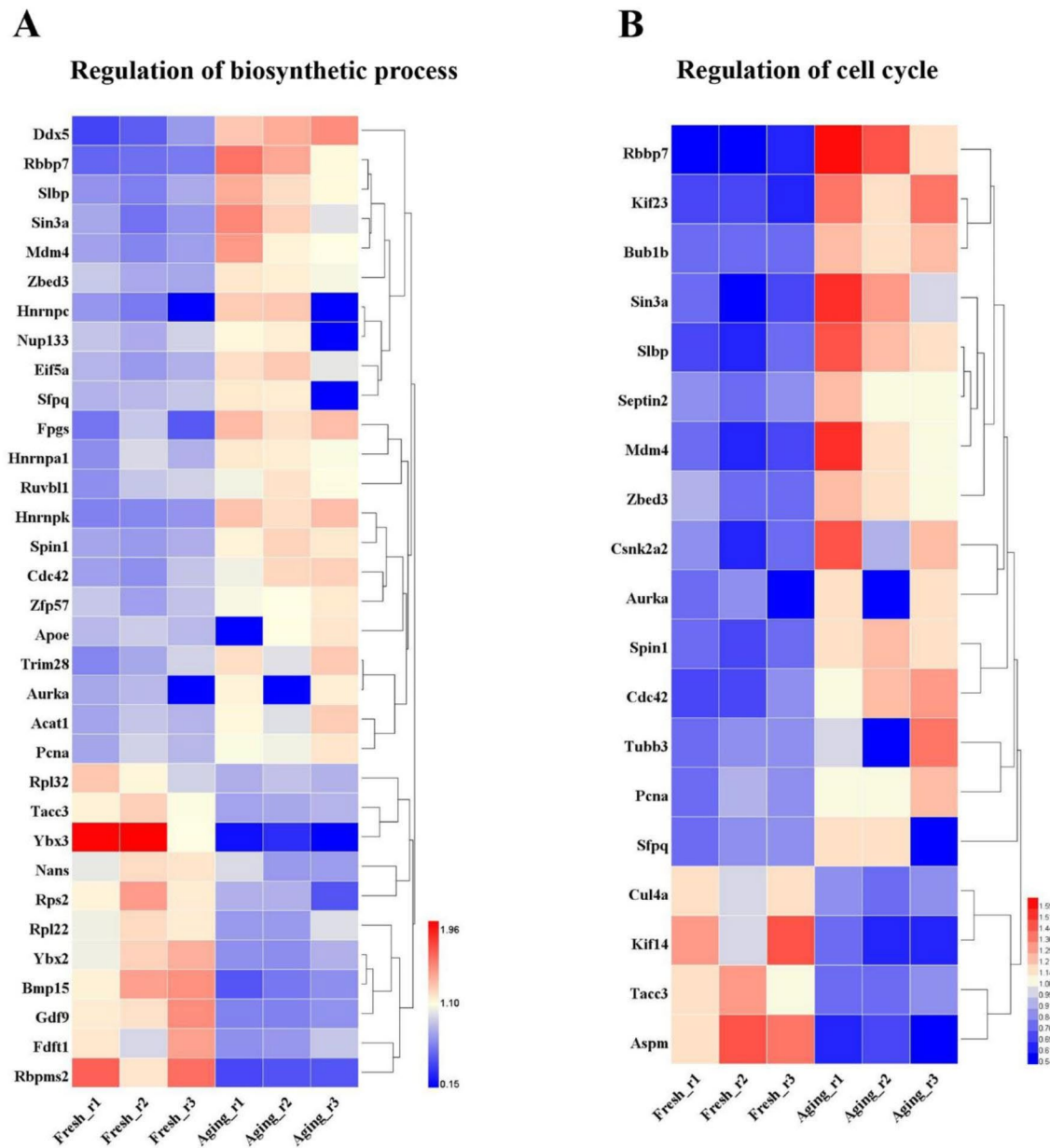


**Fig. 7** Altered regulation of biosynthetic process and cell cycle process due to postovulatory aging. **a** The heat map for the protein expression level related to the regulation of biosynthetic process. **b** The heat map for the protein expression level related to the regulation of cell cycle

unigenes respectively. The results of GO analysis showed that most DEPs were related to regulation of gene expression, biosynthetic process, RNA metabolic process and cell cycle process. Then we mainly focused on DEPs involved in these four biological processes.

Firstly, we filtrated the DEPs participated in regulation of gene expression. Conspicuously, proteins were found to be differentially expressed in regulation of each of the three major stages of gene expression, that is, transcription, translation and post-translational modifications,

which suggested that postovulatory aging affected every stage of gene expression. In the last decades, researches have manifested that postovulatory aging can disrupt the normal epigenetic configuration before and after fertilization, thus interfering with embryo epigenome and its subsequent development [31, 32]. Histone modifications are among the most crucial epigenetic factors that regulate this process [6]. Evidence showed that augment of acetylation on histones H3 and H4 as well as hypomethylation of H19 could accelerate the aging process [31, 33].

In the current study, six proteins associated with histone modification exhibited a differential expression, confirming the epigenetic variations due to postovulatory aging at the global proteomic level. Excitingly, Sin3a and Ruvbl1, both associated with histone acetylation, were significantly up-regulated. Moreover, the overexpression of another maternal-effect factor SLBP, which acts as a stabilizer of histone mRNA, could lead to an overload of histone H3 on chromosomes, resulting in chromosome excessive condensation [1, 34]. Trim 28 and Zfp57, both belong to maternal-effect proteins and act synergistically on DNA methylation of early embryo during mouse oocyte to embryo transition [35, 36], showed an increasing expression. Our results provided insights into molecular mechanisms of epigenetic abnormalities caused by postovulatory aging.

It is generally acknowledged that mammalian early embryos are transcriptionally quiescent, the development depends on maternal RNAs stored in the oocyte cytoplasm until zygotic genome activation [14, 37]. Therefore, the metabolism of RNA is critical in the mature MII oocyte before fertilization. Our research showed that proteins related to RNA alternative splicing, RNA export from nucleus and negative regulation of transcription from RNA polymerase II promoter were significantly expressed. Based on the available evidences, alternative splicing plays a key role in regulating early embryonic development, especially the transition from zygote to 2-cell stages [38, 39]. Previous research also demonstrated that the hyperphosphorylated form (HIO) of RNA polymerase II, which takes charge of transcription of mRNA in eukaryotes, was found to be colocalized with mRNA splicing proteins and operate on mRNA splicing [40]. Given that critical processing including alternative splicing of exons takes place within the nucleus and then RNAs are exported to the cytoplasm to participate in further gene expression [41], the up-regulation of RNA export-related genes may have a causality with more frequent splicing. Thereout, we speculated that abnormal alternative splicing could be one of the important reasons accounting for the decline in embryonic developmental potential of aging oocytes [42].

The healthy development of early embryos relies on the synthesis of numerous macromolecules. Our data identified 33 DEPs involved in the regulation of biosynthesis, including the biosynthetic process of coenzyme, amino acid, cofactor, nucleobase-containing compound and so on, which are all necessary and indispensable factors in the progression of embryonic development. Hence, we suspected that the disturbance in the regulation of biosynthetic process might result in the impaired developmental competency of aging oocytes.

Cell cycle regulation is considered to be one of the known mechanisms of postovulatory aging, and the

downregulation of maturation-promoting factor (MPF) and mitogen-activated protein kinase (MAPK) proteins and mitotic arrest deficient 2 (Mad2) transcript were strongly linked to the process [43, 44]. Yet the specific biochemical pathway has not been clearly elaborated. Thrilly, up to 19 DEPs identified played a part in the regulation of cell cycle, and some of these proteins are pivotal molecular assuring the proper progression of the cell cycle in oocytes. Spindlin 1 (Spin1), component of a ribonucleoprotein complex and regulates meiotic resumption in mouse oocytes [45], was overexpressed in the aging oocyte. A critical spindle checkpoint protein budding uninhibited by benzimidazole 1 (Bub1) that ensures accurate chromosome alignment and homolog separation in oocyte meiosis [46, 47] was also up-regulated in the aging oocytes. Similarly, the key acentriolar microtubule-organizing center (MTOC) constituent Aurka which plays a vital part in regulating meiotic spindle assembly in oocytes [48–50] also exhibited an increased expression pattern. The expression levels of several microtubule-associated proteins including TACC3, KIF14 and ASPM were also reduced in the aging oocytes. The results of our study will provide direction for the future in-depth study of this mechanism of postovulatory aging.

Among the DEPs screened out, five were identified oocyte-specific maternal-effect factors, namely T cell leukemia/lymphoma 1B, 1 (Tcl1b1), Slbp, Trim28, Zfp57 and zygote arrest 1 (Zar1), which affected embryonic development via different pathways and perhaps acted as a culprit in the compromised embryonic development of aging oocytes as well [36].

The limitation of our study is that we did not perform overexpression or knockdown verification of these DEPs on fresh mouse matured MII oocytes. In addition, although postovulatory aging is a relatively conserved progress among species, there are differences between the proteome of mice and humans. We used mouse oocytes to explore processes related with postovulatory aging due to the rarity of human oocyte samples, which may not absolutely mirror processes in aging human oocytes. Well-designed verification researches are demanded to further test our hypotheses.

## Conclusion

In conclusion, with the application of 4D-LFQ, this study revealed that abnormal regulation of gene expression, RNA metabolism, biosynthesis and cell cycle might all accelerate the course of postovulatory aging and lead to the decline in the developmental potential of aging mouse oocytes. These findings in mouse oocytes may, in part, explain disturbances and declined developmental potential of aging human oocytes and help to prevent postovulatory aging in vivo and in vitro. A deeper insight into these DEPs is expected to open up a new angle on

the mechanisms of postovulatory aging, providing a theoretical basis for developing viable strategies to improve natural pregnancy and ART success rates.

#### Abbreviations

2D DIGE	two-dimensional Difference Gel Electrophoresis
4D-LFQ	four-dimensional label-free quantification mass spectrometry
ASPM	abnormal spindle-like microcephaly-associated protein homolog
Aurka	aurora kinase A
Bmp15	bone morphogenetic protein 15
Bub1	benzimidazole 1
COCs	cumulus oocyte complexes
DDX5	DEAD box helicase 5
DEP	differentially expressed protein
EIF5A	eukaryotic translation initiation factor 5A-1
FDR	false discovery rate
FPKM	fragments per kilobase of transcript sequence per millions base pairs sequenced
GDF9	growth/differentiation factor 9
GO	Gene Ontology
hCG	human chorionic gonadotropin
Hnrnpa1	heterogeneous nuclear ribonucleoprotein A1
Hnrnpk	heterogeneous nuclear ribonucleoprotein K
ICR	Institute of Cancer Research
KEGG	Kyoto Encyclopedia of Genes and Genomes
KOG	eukaryote clusters of orthologous groups
Mad2	mitotic arrest deficient 2
MALDI/TOF MS	Matrix-Assisted Laser Desorption/Ionization Time of Flight/Time of Flight Mass Spectrometry
MAPK	mitogen-activated protein kinase
Mdm4	transformed mouse 3T3 cell double minute 4
MII	metaphase II
MPF	maturation-promoting factor
MS	mass spectrum
MTOC	acentriolar microtubule-organizing center
MTX2	metaxin-2
NCBI	National Center for Biotechnology Information
Nup133	nucleoporin 133
PASEF	parallel accumulation serial fragmentation
Pcna	proliferating cell nuclear antigen
PMSG	pregnant mare serum gonadotropin
RBBP7	retinoblastoma binding protein 7, chromatin remodeling factor
Ruvb1	RuvB-like 1
SEM	standard error of mean
Sfpq	splicing factor proline/glutamine rich
Sin3a	transcriptional regulator, SIN3A
SLBP	stem-loop binding protein
Spin1	Spindlin 1
TACC3	transforming acidic coiled-coil-containing protein 3
Tcl1b1	T cell leukemia/lymphoma 1B, 1
TGFβ	transforming growth factor-beta
timsTOF	Protome-of-flight mass spectrometer
Trim28	tripartite motif-containing 28
Ybx2	Y-box-binding protein 2
Ybx3	Y-box-binding protein 3
Zar1	zygote arrest 1
Zfp57	zinc finger protein 57

#### Supplementary Information

The online version contains supplementary material available at <https://doi.org/10.1186/s13048-022-01045-6>.

Supplementary Material 1: Table S1. Detail information of all MS identified proteins and peptides.

#### Acknowledgements

We would like to thank for the sequencing platform and bioinformation analysis of PTM Biolabs Inc. (Hangzhou, China)

#### Authors' contributions

KW and CZ designed the study, CZ and XD carried out the analysis and interpretation of data and wrote the manuscript, XY, JS and JW performed the experiments. KW and BL supervised the project. All the authors approved the final version of manuscript.

#### Funding

This research was supported by the National Natural Science Foundation of China (32170817) and the Fundamental Research Funds of Shandong University.

#### Data Availability

MS data will be uploaded to pubmed if this manuscript was accepted. All other data that support the findings of this study are available from the corresponding authors upon reasonable request.

#### Declarations

##### Ethics approval

All the procedures in this study were audited and confirmed by the Ethic Committee of Reproductive Medicine of Reproductive Hospital of Shandong University (2021-15). And all experiments conducted complied with relative rules and regulations of the committees.

##### Consent for publication

Not applicable.

##### Competing interests

The authors declare that they have no competing interests.

Received: 7 June 2022 / Accepted: 16 September 2022

Published online: 14 October 2022

#### References

- Miao YL, Kikuchi K, Sun QY, Schatten H. Oocyte aging: cellular and molecular changes, developmental potential and reversal possibility. *Hum Reprod Update*. 2009;15(5):573–85.
- Jia B-Y, Xiang D-C, Shao Q-Y, Zhang B, Liu S-N, Hong Q-H, et al. Inhibitory effects of astaxanthin on postovulatory porcine oocyte aging in vitro. *Sci Rep*. 2020;10(1):20217.
- Fissore RA, Kurokawa M, Knott J, Zhang M, Smyth J. Mechanisms underlying oocyte activation and postovulatory ageing. *Reproduction*. 2002;124(6):745–54.
- Wilcox AJ, Weinberg CR, Baird DD. Post-ovulatory ageing of the human oocyte and embryo failure. *Hum Reprod*. 1998;13(2):394–7.
- Lord T, Aitken RJ. Oxidative stress and ageing of the post-ovulatory oocyte. *Reprod (Cambridge England)*. 2013;146(6):R217–R27.
- Di Nisio V, Antonouli S, Damdimopoulou P, Salumets A, Cecconi S. In vivo and in vitro postovulatory aging: when time works against oocyte quality? *J Assist Reprod Genet*. 2022;39(4):905–18.
- Lord T, Nixon B, Jones KT, Aitken RJ. Melatonin prevents postovulatory oocyte aging in the mouse and extends the window for optimal fertilization in vitro. *Biol Reprod*. 2013;88(3):67.
- Trapphoff T, Heiligentag M, Dankert D, Demond H, Deutsch D, Frohlich T, et al. Postovulatory aging affects dynamics of mRNA, expression and localization of maternal effect proteins, spindle integrity and pericentromeric proteins in mouse oocytes. *Hum Reprod*. 2016;31(1):133–49.
- Prasad S, Tiwari M, Koch B, Chaube SK. Morphological, cellular and molecular changes during postovulatory egg aging in mammals. *J Biomed Sci*. 2015;22:36.
- Miao Y, Zhou C, Cui Z, Zhang M, ShiYang X, Lu Y, et al. Postovulatory aging causes the deterioration of porcine oocytes via induction of oxidative stress. *FASEB J*. 2018;32(3):1328–37.
- Premkumar KV, Chaube SK. An insufficient increase of cytosolic free calcium level results postovulatory aging-induced abortive spontaneous egg activation in rat. *J Assist Reprod Genet*. 2013;30(1):117–23.
- Dankert D, Demond H, Trapphoff T, Heiligentag M, Rademacher K, Eichenlaub-Ritter U, et al. Pre- and postovulatory aging of murine oocytes affect the

- transcript level and poly(A) tail length of maternal effect genes. *PLoS ONE*. 2014;9(10):e108907.
13. Trapphoff T, Heiligentag M, Dankert D, Demond H, Deutsch D, Fröhlich T, et al. Postovulatory aging affects dynamics of mRNA, expression and localization of maternal effect proteins, spindle integrity and pericentromeric proteins in mouse oocytes. *Hum Reprod (Oxford England)*. 2016;31(1):133–49.
  14. Gao Y, Liu X, Tang B, Li C, Kou Z, Li L, et al. Proteomic analysis of Mouse Embryos during Pre-implantation Development. *Cell Rep*. 2017;21(13):3957–69.
  15. Vogel C, Marcotte EM. Insights into the regulation of protein abundance from proteomic and transcriptomic analyses. *Nat Rev Genet*. 2012;13(4):227–32.
  16. Pfeiffer MJ, Taher L, Drexler H, Suzuki Y, Makalowski W, Schwarzer C, et al. Differences in embryo quality are associated with differences in oocyte composition: a proteomic study in inbred mice. *Proteomics*. 2015;15(4):675–87.
  17. Yang S, Wei Z, Wu J, Sun M, Ma Y, Liu G. Proteomic analysis of liver tissues in chicken embryo at Day 16 and Day 20 reveals antioxidant mechanisms. *J Proteom*. 2021;243:104258.
  18. Meier F, Brunner AD, Koch S, Koch H, Lubeck M, Krause M, et al. Online Parallel Accumulation-Serial Fragmentation (PASEF) with a Novel Trapped Ion Mobility Mass Spectrometer. *Mol Cell Proteomics*. 2018;17(12):2534–45.
  19. Brzhozovskiy A, Kononikhin A, Bugrova AE, Kovalev GI, Schmit PO, Kruppa G, et al. The Parallel Reaction Monitoring-Parallel Accumulation-Serial Fragmentation (prM-PASEF) Approach for Multiplexed Absolute Quantitation of Proteins in Human Plasma. *Anal Chem*. 2022;94(4):2016–22.
  20. Akkurt Arslan M, Kolman I, Pionneau C, Chardonnet S, Magny R, Baudouin C, et al. Proteomic Analysis of Tears and Conjunctival Cells Collected with Schirmer Strips Using timsTOF Pro: Preanalytical Considerations. *Metabolites*. 2021;12(1).
  21. Hamada S, Pionneau C, Parizot C, Silvie O, Chardonnet S, Marinach C. In-depth proteomic analysis of *Plasmodium berghei* sporozoites using trapped ion mobility spectrometry with parallel accumulation-serial fragmentation. *Proteomics*. 2021;21(6):e2000305.
  22. Christou-Kent M, Dhellemmes M, Lambert E, Ray PF, Arnoult C. Diversity of RNA-Binding Proteins Modulating Post-Transcriptional Regulation of Protein Expression in the Maturing Mammalian Oocyte. *Cells*. 2020;9(3).
  23. Xu R, Li C, Liu X, Gao S. Insights into epigenetic patterns in mammalian early embryos. *Protein & Cell*. 2021;12(1).
  24. Sayers EW, Beck J, Bolton EE, Bourexis D, Brister JR, Canese K, et al. Database resources of the National Center for Biotechnology Information. *Nucleic Acids Res*. 2021;49(D1):D10–D7.
  25. Nadendla S, Jackson R, Munro J, Quaglia F, Mészáros B, Olley D, et al. ECO: the Evidence and Conclusion Ontology, an update for 2022. *Nucleic Acids Res*. 2022;50(D1):D1515–D21.
  26. Demond H, Trapphoff T, Dankert D, Heiligentag M, Grümmer R, Horsthemke B, et al. Preovulatory Aging In Vivo and In Vitro Affects Maturation Rates, Abundance of Selected Proteins, Histone Methylation Pattern and Spindle Integrity in Murine Oocytes. *PLoS ONE*. 2016;11(9):e0162722.
  27. Thompson JG. The impact of nutrition of the cumulus oocyte complex and embryo on subsequent development in ruminants. *J Reprod Dev*. 2006;52(1):169–75.
  28. Ruebel ML, Latham KE. Listening to mother: Long-term maternal effects in mammalian development. *Mol Reprod Dev*. 2020;87(4):399–408.
  29. Yu H, Wang Y, Wang M, Liu Y, Cheng J, Zhang Q. Growth differentiation factor 9 (gdf9) and bone morphogenetic protein 15 (bmp15) are potential intraovarian regulators of steroidogenesis in Japanese flounder (*Paralichthys olivaceus*). *Gen Comp Endocrinol*. 2020;297:113547.
  30. Jiang G-J, Wang K, Miao D-Q, Guo L, Hou Y, Schatten H, et al. Protein profile changes during porcine oocyte aging and effects of caffeine on protein expression patterns. *PLoS ONE*. 2011;6(12):e28996.
  31. Huang JC, Yan LY, Lei ZL, Miao YL, Shi LH, Yang JW, et al. Changes in histone acetylation during postovulatory aging of mouse oocyte. *Biol Reprod*. 2007;77(4):666–70.
  32. Sun Y-L, Tang S-B, Shen W, Yin S, Sun Q-Y. Roles of Resveratrol in Improving the Quality of Postovulatory Aging Oocytes In Vitro. *Cells*. 2019;8(10).
  33. Liang XW, Ge ZJ, Wei L, Guo L, Han ZM, Schatten H, et al. The effects of postovulatory aging of mouse oocytes on methylation and expression of imprinted genes at mid-term gestation. *Mol Hum Reprod*. 2011;17(9):562–7.
  34. Jin Y, Yang M, Gao C, Yue W, Liang X, Xie B, et al. Fbxo30 regulates chromosome segregation of oocyte meiosis. *Cell Mol Life Sci*. 2019;76(11):2217–29.
  35. Messerschmidt DM, de Vries W, Ito M, Solter D, Ferguson-Smith A, Knowles BB. Trim28 is required for epigenetic stability during mouse oocyte to embryo transition. *Science (New York)*. 2012;335(6075):pp.1499–502.
  36. Condic ML. The Role of Maternal-Effect Genes in Mammalian Development: Are Mammalian Embryos Really an Exception? *Stem Cell Reviews and Reports*. 2016;12(3):276–84.
  37. Wassarman PM, Kinloch RA. Gene expression during oogenesis in mice. *Mutat Res*. 1992;296:1–2.
  38. Revil T, Gaffney D, Dias C, Majewski J, Jerome-Majewska LA. Alternative splicing is frequent during early embryonic development in mouse. *BMC Genomics*. 2010;11:399.
  39. Xing Y, Yang W, Liu G, Cui X, Meng H, Zhao H, et al. Dynamic Alternative Splicing During Mouse Preimplantation Embryo Development. *Front Bioeng Biotechnol*. 2020;8:35.
  40. Memili E, First NL. Developmental changes in RNA polymerase II in bovine oocytes, early embryos, and effect of alpha-amanitin on embryo development. *Mol Reprod Dev*. 1998;51(4):381–9.
  41. van der Graaf K, Jindrich K, Mitchell R, White-Cooper H. Roles for RNA export factor, Nxt1, in ensuring muscle integrity and normal RNA expression in *Drosophila*. *G3 (Bethesda, Md)*. 2021;11(1).
  42. Li M, Ren C, Zhou S, He Y, Guo Y, Zhang H, et al. Integrative proteome analysis implicates aberrant RNA splicing in impaired developmental potential of aged mouse oocytes. *Aging Cell*. 2021;20(10):e13482.
  43. Abbott AL, Xu Z, Kopf GS, Ducibella T, Schultz RM. In vitro culture retards spontaneous activation of cell cycle progression and cortical granule exocytosis that normally occur in in vivo unfertilized mouse eggs. *Biol Reprod*. 1998;59(6):1515–21.
  44. Steuerwald NM, Steuerwald MD, Mailhes JB. Post-ovulatory aging of mouse oocytes leads to decreased MAD2 transcripts and increased frequencies of premature centromere separation and anaphase. *Mol Hum Reprod*. 2005;11(9):623–30.
  45. Choi J-W, Zhao M-H, Liang S, Guo J, Lin Z-L, Li Y-H, et al. Spindlin 1 is essential for metaphase II stage maintenance and chromosomal stability in porcine oocytes. *Mol Hum Reprod*. 2017;23(3):166–76.
  46. Yin S, Wang Q, Liu J-H, Ai J-S, Liang C-G, Hou Y, et al. Bub1 prevents chromosome misalignment and precocious anaphase during mouse oocyte meiosis. *Cell Cycle (Georgetown Tex)*. 2006;5(18):2130–7.
  47. McGuinness BE, Anger M, Kouznetsova A, Gil-Bernabe AM, Helmhart W, Kudo NR, et al. Regulation of APC/C activity in oocytes by a Bub1-dependent spindle assembly checkpoint. *Curr Biol*. 2009;19(5):369–80.
  48. Kinoshita K, Noetzel TL, Pelletier L, Mechtler K, Drechsel DN, Schwager A, et al. Aurora A phosphorylation of TACC3/maskin is required for centrosome-dependent microtubule assembly in mitosis. *J Cell Biol*. 2005;170(7):1047–55.
  49. Nguyen AL, Schindler K. Specialize and Divide (Twice): Functions of Three Aurora Kinase Homologs in Mammalian Oocyte Meiotic Maturation. *Trends Genet*. 2017;33(5):349–63.
  50. Wang X, Baumann C, De La Fuente R, Viveiros MM. CEP215 and AURKA regulate spindle pole focusing and aMTOC organization in mouse oocytes. *Reprod (Cambridge England)*. 2020;159(3):261–74.

## Publisher's Note

Springer Nature remains neutral with regard to jurisdictional claims in published maps and institutional affiliations.